Quantitative PET Imaging of Bone Marrow Glucose Metabolic Response to Hematopoietic Cytokines

Wei-Jen Yao, Carl K. Hoh, Randall A. Hawkins, John A. Glaspy, Jeffrey A. Weil, Shay J. Lee, Jamshid Maddahi and Michael E. Phelps

Division of Nuclear Medicine and Biophysics, Department of Molecular and Medical Pharmacology, Laboratory of Structural Biology and Molecular Medicine (DOE), The Crump Institute for Biological Imaging; and Division of Hematology and Oncology, Department of Medicine, UCLA School of Medicine, Los Angeles, California

To evaluate the effects of hematopoietic cytokines on bone marrow glucose metabolism noninvasively, we studied serial quantitative FDG-PET images in 18 patients with metastatic melanoma and normal bone marrow who were undergoing granulocyte-macrophage colony-stimulating factor (GMCSF) or macrophage colony-stimulating factor (MCSF) administration as an adjunct to chemotherapy. **Methods:** All patients received 14 days of cytokine therapy in three groups: four patients were treated with GMCSF (5 μg/kg/d SQ), eight patients were treated with GMCSF (5 μg/kg/d SQ) and monoclonal antibody (MAbR24) and six patients were treated with MCSF (80 μg/kg/d IVCI) and MAbR24. Dynamic FDG-PET imaging was performed over the lower thoracic or upper lumbar spine at four time points in each patient. **Results:** Baseline glucose metabolic rates in the bone marrow of these three groups of patients were similar (5.2 ± 0.7, 4.4 ± 0.8 and 4.8 ± 1.2 μg/min/g as mean value and standard deviations, respectively). In both GMCSF and GMCSF + R24 groups, rapid increases in bone marrow glucose metabolic rates were observed during therapy. After GMCSF was stopped, bone marrow glucose metabolic rates rapidly decreased in both groups. The glucose metabolic response in these two groups was not significantly different by pooled t-statistics ($p = 0.105$). In the MCSF + R24 group, the increase of glucose metabolic rate on Days 3 and 10 was 35% and 31% above baseline on the average, but was not significant. **Conclusion:** The results support the use of parametric FDG-PET imaging for noninvasive quantitation of bone marrow glucose metabolic changes to hematopoietic cytokines in vivo.

Key Words: fluorine-18-fluorodeoxyglucose; positron emission tomography; bone marrow; glucose metabolism; hematopoietic growth factors

J Nucl Med 1995; 36:794–799

Hematopoietic cytokines, such as granulocyte-macrophage colony-stimulating factor (GMCSF) and macrophage colony-stimulating factor (MCSF), are a family of glycoprotein growth factors that have potent effects in stimulating proliferation, differentiation and survival of hematopoietic progenitor cells in the bone marrow (*1–3*). GMCSF has been mass-produced with recombinant technology and has been used increasingly for preventing patients from developing myelosuppressive effects of radiation and chemotherapy (*4*). Furthermore, in the appropriate setting, it may also augment the antineoplastic effect in some solid tumors by increasing the number of circulating effector cells and by enhancing granulocyte antibody-dependent cellular cytotoxicity (*5*).

In vivo studies have demonstrated that GMCSF and MCSF can elevate glucose utilization of immune-competent tissues and whole-body glucose turnover due to a marked glucose metabolic response of polymorphonuclear cells and macrophages after GMCSF and MCSF injection (*6,7*). With PET, biochemical imaging can be performed, allowing noninvasive, in vivo quantitative assessment of glucose metabolic rate in various tissues using ^{18}F-fluorodeoxyglucose (FDG). PET with FDG was first utilized in humans to quantify cerebral glucose metabolism (*8,9*), based on a tracer kinetic method developed by Sokoloff et al. (*10*). Because of the high glycolic rate of many malignancies (*11*), quantitative FDG-PET imaging has been employed to detect the presence of malignant tissues (*12–18*) and to quantify changes in tumor glycolysis during and after treatment (*19–22*).

We hypothesized that the FDG-PET method can demonstrate changes in glucose metabolic rate of bone marrow after cytokine therapy. In this study, we performed serial kinetic bone marrow FDG-PET scans in patients with metastatic melanoma who were undergoing GMCSF or MCSF administration as an adjunct to chemotherapy to assess the effect of cytokines on bone marrow glucose metabolism.

Received Mar. 31, 1994; revision accepted Oct. 18, 1994.
For correspondence or reprints contact: Carl K. Hoh, MD, UCLA Medical School, CHS AR-128, 10833 Leconte Ave., Los Angeles, CA 90024-6942.

TABLE 1
Baseline Characteristics of 18 Patients with Metastatic Melanoma in Different Protocols

	GMCSF	GMCSF + R24	MCSF + R24
Number of patients	4	8	6
Age (yr)	55 ± 18	47 ± 8	57 ± 11
Gender (M,F)	3,1	4,4	3,3
Therapy regimen	GMCSF (5 μg/kg/d SQ) * 14 d	GMCSF (5 μg/kg/d SQ) * 14 d and R24 * 7D (Days 4 to 10)	MCSF (80 μg/kg/d IVIC) * 14 d and R24 * 7D (Days 4 to 10)
Bone marrow GMR (μg/min/g)	5.2 ± 0.7	4.4 ± 0.8	4.8 ± 1.2

GMR = glucose metabolic rate; values are mean and standard deviation.

MATERIALS AND METHODS

Patients and Treatment Regimen

The study group consisted of 18 patients with biopsy-proven metastatic melanoma and without evidence of bone marrow metastases who were part of a clinical protocol for assessing the efficacy of various chemotherapeutic regimens and who also underwent serial dynamic FDG-PET imaging of the thoraco-lumbar region. All patients received 14 days of GMCSF or MCSF as adjunctive treatment with different chemotherapeutic protocols: four patients were treated with GMCSF (5 μg/kg/d SQ) alone during the period of study, eight patients were treated with GMCSF (5 μg/kg/d SQ) and monoclonal antibody (MabR24, from Day 4 to Day 10) and six patients were treated with MCSF (80 μg/kg/d IVCI) and MabR24 (from Day 4 to Day 10). All patients gave informed consent; the study protocol was approved by the UCLA Human Subject Protection Committee.

Image Acquisition

Dynamic FDG-PET imaging was performed over the lower thoracic or upper lumbar spine regions at four time points: 3 days prior to cytokine therapy, 3 days and 10 days during therapy, and 3 days after therapy. The patients were positioned supine with two pillows under the patient's knee for comfort and for straightening the lumbar curvature of the spine.

Following intravenous injection of 10 mCi of FDG, dynamic images were acquired with a Siemens/CTI 931/08 (Knoxville, TN) tomograph. The device simultaneously acquired eight cross-sectional images, each 6.75 mm thick, with a total axial field of view of 10.8 cm. A 20-min transmission scan was obtained using a $^{68}Ge/^{68}Ga$ external ring source in order to correct for photon attenuation effect. The dynamic sequence consisted of twelve 10-second scans, four 30-second scans and fourteen 240-second scans for a total scan time of 60 min. Cross-sectional images were reconstructed using a Shepp-Logan filter with a cutoff frequency of 0.30 Nyquist frequency, yielding an in-plane spatial resolution of 10 mm FWHM. From a dorsal hand vein, heated to 44°C to arterialize blood, 2-ml blood samples were taken at 5–10-sec intervals over the first 3 min and at progressively lengthening intervals over the duration of the study (*8*). Assays of ^{18}F plasma concentrations were performed in a NaI well counter after centrifugation of the blood samples. A cylinder phantom filled with $^{68}Ge/^{68}Ga$ solution was scanned on the same day of the PET study to determine the conversion factor between image data in units of counts/pixel/sec and well counter data in units of counts/ml/sec.

Patients' plasma glucose concentrations were determined using a quantitative enzymatic (hexakinase) assay before tracer injection and at 15, 30, 45 and 60 min during imaging of each study.

Calculation of Bone Marrow Glucose Metabolic Rate

Patlak graphical analysis was used to generate parametric images of the rate constant Kpat (ml/min/g) for net phosphorylation of FDG as reported previously (*23*). A good correlation between K values from nonlinear regression and from Patlak graphical analysis has been reported in metastatic melanoma lesions (*24*).

Regions of interest (ROIs) were drawn over the vertebral bodies. The ROI size and anatomic location were determined based on the post-treatment transaxial PET images, which had generally higher bone marrow glucose metabolism, and were correlated with the anatomical location shown on CT. Average ROI counts were obtained by averaging ROI counts from each vertebral body demonstrated in the PET images. In each patient, identical ROIs were used for repeat studies by applying the ROI from the post-treatment image to the baseline image. To identify the location of bone marrow in those patients with very low baseline bone marrow activity, the post-treatment PET images were registered to the baseline image using a previously described method (*25*). This allowed selection of identical ROIs on serial studies.

The glucose metabolic rate (μg/min/g) of bone marrow was calculated according to Huang et al. (*9*):

$$\text{glucose metabolic rate} = K_{pat} * C_p/LC,$$

where K_{pat} is the average K value of bone marrow from parametric images, C_p is the mean plasma glucose concentration throughout the image acquisition and LC is the lumped constant, which accounts for the differences in the transport and phosphorylation of FDG and glucose and was assumed to be 1.0 for bone marrow and remained constant in this study.

Statistical Analysis

Repeated measures analysis of variance and t-tests for unpaired samples were used. Statistical significance was indicated at the 5% level.

RESULTS

The baseline characteristics of the study population are listed in Table 1. There were four patients in the GMCSF group, eight patients in the GMCSF + R24 group and six patients in the MCSF + R24 group. The baseline bone marrow glucose metabolic rates were similar in these three groups (5.2 ± 0.7 μg/min/g, 4.4 ± 0.8 μg/min/g and 4.8 ± 1.2 μg/min/g, respectively).

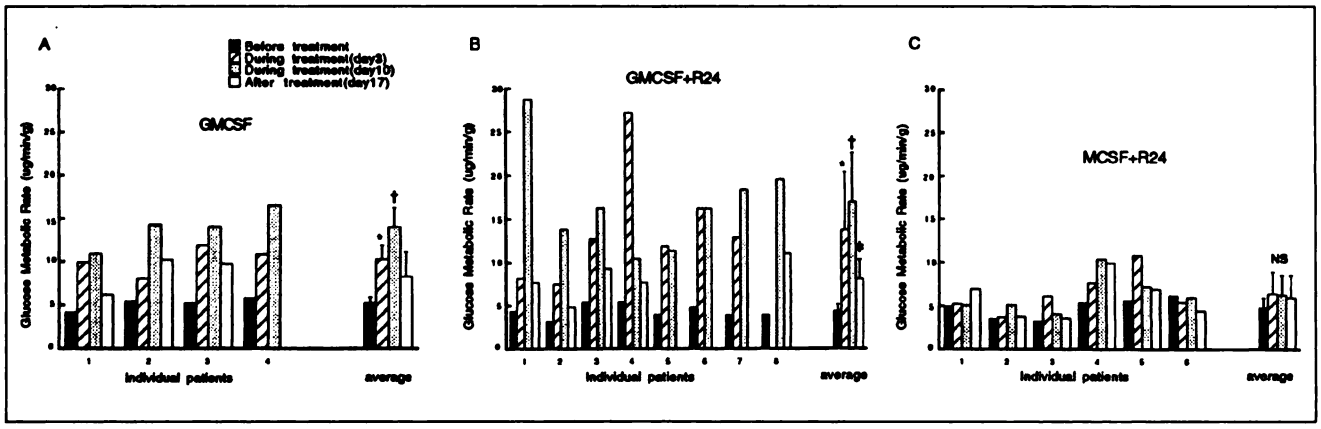

FIGURE 1. Glucose metabolic rate (μg/min/g) of bone marrow before, during and after cytokine treatment in different groups. Individual and average glucose metabolic rates in GMCSF (n = 4), GMCSF + R24 (n = 8) and MCSF + R24 (n = 6) groups are represented in graphs A, B and C, respectively. *p < 0.01, †p < 0.001, ‡p < 0.05. NS = not significant compared to glucose metabolic rates on Day 0.

Effect of GMCSF on Bone Marrow Glucose Metabolic Rate

Alteration of bone marrow glucose metabolic rate before, during and after GMCSF therapy is presented in Figure 1A. During GMCSF therapy, all four patients showed rapid increase of bone marrow glucose metabolic rate from a baseline of 5.2 ± 0.7 μg/min/g to 10.2 ± 1.7 μg/min/g on Day 3 (97% increase, $p < 0.01$) and continued increase to 14.0 μg/min/g on Day 10 (170% increase, $p < 0.001$). Three days after discontinuation of GMCSF, three patients had a rapid fall of bone marrow glucose metabolic rate to 8.3 ± 0.29 μg/min/g (60% increase above baseline). Patient 4 did not complete this study.

Effect of GMCSF + R24 on Bone Marrow Glucose Metabolic Rate

The bone marrow response to GMCSF + R24 during therapy (Fig. 1B) showed a similar pattern but with a higher increase in the glucose metabolic rate as compared to the GMCSF group. The average glucose metabolic rate was increased from 4.4 ± 0.8 μg/min/g at baseline to 13.8 ± 6.5 μg/min/g on Day 3 (215% increase, $p < 0.01$) and 16.8 ± 5.8 μg/min/g on Day 10 (285% increase, $p < 0.001$). Despite some variation in the degree of response among patients, all patients receiving GMCSF + 24 therapy had rapid and significant increases in bone marrow glucose metabolic rate on Day 3 during therapy (varied from 90% to 403% increase). On Day 10 of therapy, five patients showed continued increase of glucose metabolic rate, two patients (Patients 5 and 6) remained at the same level and one patient (Patient 4) showed a reduction of glucose metabolic rate compared to Day 3. After GMCSF was stopped, all five patients completing this study showed rapid decreases in the glucose metabolic rate, but still significantly higher than baseline levels (86% increase, $p < 0.05$). On visual inspection, hypermetabolic bone marrow could be observed in the vertebral bodies, ribs and sternum in all patients on Days 3 and 10 after GMCSF administration. The uptake pattern was homogeneous and symmetrical in distribution (Fig. 2).

Effect of MCSF + R24 on Bone Marrow Glucose Metabolic Rate

In the six patients receiving MCSF + R24, the average bone marrow glucose metabolic rate was increased from 4.8 ± 1.2 μg/min/g to 6.5 ± 2.5 μg/min/g on Day 3 (35%

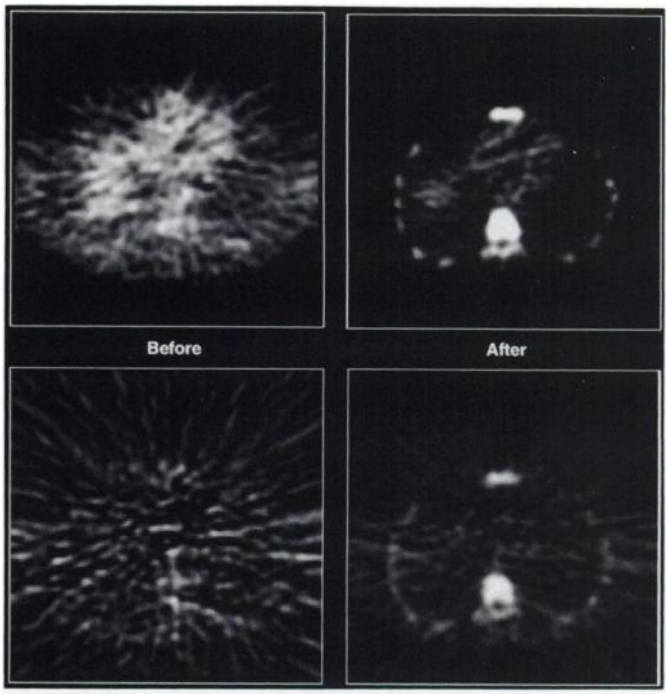

FIGURE 2. Transaxial FDG-PET images of the lower thoracic region before (left) and after (right) GMCSF administration in Patient 4 of the GMCSF + R24 group. Unprocessed dynamic images from 48–60 min after FDG injection are in the upper row; parametric images are in the lower row. After GMCSF administration, striking bone marrow glucose metabolism is demonstrated in the vertebral body, ribs and sternum. Notice the cardiac blood pool and right liver dome activity are suppressed in the parametric images since FDG uptake in these organs does not follow the Patlak model.

TABLE 2
Effects of Different Protocols on Glucose Metabolic Rate in Bone Marrow

Group	Baseline	During therapy		After therapy
	Day 0	Day 3	Day 10	Day 17
GMCSF	5.2 ± 0.7	10.2 ± 1.7 (97)*	14.0 ± 2.3 (170)†	8.3 ± 2.9 (60)
GMCSF + R24	4.4 ± 0.8	13.8 ± 6.6 (215)*	16.9 ± 5.7 (285)†	8.1 ± 2.3 (86)‡
MCSF + R24	4.8 ± 1.2	6.5 ± 2.5 (35)	6.3 ± 2.3 (31)	6.0 ± 2.6 (24)

*$p < 0.01$, †$p < 0.001$, ‡<0.05; vs. Day 0.
Values are glucose metabolic rates in μg/min/g for means ± s.d. (% increase).

increase) and 6.3 ± 2.3 μg/min/g on Day 10 (31% increase) after injection of MCSF, but this was not significant (Fig. 1C). Alterations of glucose metabolic rate among these patients varied from 12% below to 93% above baseline on Day 3, and 4% below to 93% above baseline on Day 10. Three patients showed a slight increase in bone marrow glucose metabolic rates during therapy (Patients 3, 4 and 5), while three patients had no change (Patients 1, 2 and 6).

Comparison of Bone Marrow Glucose Metabolic Response between Groups

The effect of different protocols on average bone marrow glucose metabolic rate in the three groups is summarized in Table 2. In both GMCSF and GMCSF + R24 groups, a rapid and significant increase in bone marrow glucose metabolic rate on Day 3 (97% and 215% increase, respectively, $p < 0.01$) and a continued increase on Day 10 (170% and 285%, respectively, $p < 0.001$) during therapy as noted. Patients treated with GMCSF + R24 had higher glucose metabolic rates than with GMCSF during therapy (215% increase versus 97% increase on Day 3 and 285% increase versus 170% increase on Day 10). A pooled t-statistic was used to test for differences between GMCSF versus GMCSF + R24 groups on Day 10. This difference was not significant ($p = 0.105$). Three days after discontinuation of GMCSF, bone marrow glucose metabolic rates decreased rapidly toward baseline levels, dropping from 170% to 60% above baseline in the GMCSF group, and dropping from 285% to 86% above baseline in the GMCSF + R24 group. In the MCSF group, the increase of glucose metabolic rate on Days 3 and 10 averaged 35% and 31% above baseline, respectively, but did not attain statistical significance at the $p < 0.05$ level.

DISCUSSION

PET is demonstrating an increasingly important role in the understanding of human biochemistry. Over the past decade, PET has been used to elucidate numerous biological processes noninvasively. PET with FDG has proved to be valuable for the noninvasive assessment of organ glucose metabolism, primarily in the brain and heart, and a wide variety of tumors. The rapidly increasing use of PET and FDG in whole-body imaging to identify, grade and stage tumors prior to and following therapy has caused investigators to examine the normal or abnormal metabolism of glucose throughout all organ systems of the body. In the present study, we showed glucose metabolic alterations occurring in the bone marrow of 18 patients who received GMCSF or MCSF as adjunctive therapy for metastatic melanoma.

We observed an increase in bone marrow glucose metabolic rates by 170% and 285% on Day 10 during GMCSF administration in the GMCSF and GMCSF + R24 groups, respectively. Although not proven in this study, increased bone marrow glucose metabolic rates could be explained by an increased proliferation of bone marrow cells. This is supported by in vivo studies which showed an increase of bone marrow cellularity with a marked preponderance of neutrophilic and eosinophilic precursors during GMCSF therapy in patients with refractory anemia (*26*) and in patients with solid tumors (*27*). GMCSF produced a 3–5-fold increase in circulating leukocytes and a marked increase in the proportion of immature cells and the leuko-erythrogenetic ratio in bone marrow. Quantitative estimation of GMCSF effects showed that GMCSF increased the birth rate of bone marrow cycling cells from 1.3 to 3.4 cells/hr.

Although not statistically significant, bone marrow glucose metabolic rates in patients treated with GMCSF + R24 tended toward higher values than with GMCSF alone. It is possible that the monoclonal antibody MAbR24 could have contributed to the bone marrow glucose response in these patients. This effect, however, was not apparent during the study period.

We also observed a rapid "on-off" profile change in bone marrow glucose metabolic rate after GMCSF administration. A rapid increase in bone marrow glucose metabolic rates was observed 3 days after initiation of GMCSF injection followed by a persistent increase 10 days and rapid decrease 3 days after discontinuation of GMCSF. The pattern is very similar to in vivo studies using recombinant GMCSF in patients with solid tumors (*27*) and with AIDS (*28*), which showed an increase in circulating leukocyte count in the same rapid on-off profile. In their observations, the leukocyte count returned to approximate baseline levels in all patients within 3 days when GMCSF was discontinued, probably due to a sudden drop of proliferative activity of bone marrow elements. Indeed, they found that 48 to 96 hr after discontinuation of GMCSF, the proportion of S-phase blood marrow progenitors rapidly

dropped to values lower than baseline levels. In this study, however, the increase in bone marrow glucose metabolic rates was sustained longer. Three days after discontinuation of GMCSF, there was still a 60% and 86% increase in glucose metabolic rates in bone marrow in the GMCSF and GMCSF + R24 groups, respectively. In four patients receiving GMCSF + R24 therapy, bone marrow glucose metabolic rates remained significantly higher than baseline levels 22 to 34 days after administration of GMCSF and returned to approximate baseline levels at 42–45 days (data not shown). This suggests that for follow-up PET imaging, there may be significant residual bone marrow glucose metabolic response up to 4 wk after stopping GMCSF therapy.

The glucose metabolic rate in the MCSF group was not significantly different than baseline values. A lower response and small sample size may have contributed to the nonsignificance. The possible biological influence of MCSF would require additional patients for study.

There has been a good deal of uncertainty as to which cells are involved by these two cytokines due to the heterogeneity of marrow populations and the difficulty in obtaining pure populations for study. In vitro findings have indicated that GMCSF is a multilineage stimulator for progenitor cells of granulocyte, monocyte-macrophage and eosinophil colonies (*27*), whereas MCSF only stimulates the growth of monocyte-macrophage progenitors. In normal adult bone marrow, granulocytes and their precursors are predominant (about 60% of hematopoietic cells) compared to monocyte-macrophages (2%–5%). This could explain the significant increase in bone marrow glucose metabolic rates during GMCSF therapy compared to a more modest response during MCSF therapy.

Although the argument can be made that the increase in bone marrow activity could be the progression of bone marrow metastases, it is unlikely because of:

1. A previously normal PET study.
2. The rapid increase in glucose metabolic rates within days.
3. A history of cytokine therapy.
4. Diffuse distribution of hypermetabolic bone marrow.
5. Normal corresponding CT findings without evidence of bone metastases.
6. Rapid decrease in glucose metabolic rates after stopping cytokines.

With the increasing use of cytokines in cancer patients and FDG-PET in oncology, hypermetabolic bone marrow may be observed more frequently and should not be misinterpreted as bone marrow metastases. This can be easily differentiated because cytokine response is diffuse, but this will produce an increase in background activity for identification of metastatic foci.

Hypermetabolic bone marrow also has been reported in ^{201}Tl scanning (*29*), ^{99m}Tc-MDP bone scanning (*30*) and ^{99m}Tc-colloid scanning (*31*) during cytokine therapy. Recent MRI studies of the effects of cytokine on bone marrow have revealed dramatic intensity changes in the bone marrow on MR images after cytokine infusion. These changes correlated with histologic findings of replacement of fatty marrow by hematopoietic marrow containing numerous granulocytes (*32*). Different mechanisms may be involved with these imaging findings and further study for their frequency and timing is necessary.

CONCLUSION

Quantification of biological processes with PET imaging provides a means for directly measuring metabolic and biochemical abnormalities as well as assessing treatment responses in humans. We demonstrated alterations of bone marrow glucose metabolic response to hematopoietic cytokines on FDG-PET images. GMCSF can induce a significant increase in glucose metabolic rates in bone marrow, whereas MCSF had only a slight effect. In using PET and FDG to quantify metabolic changes of malignant tumors after chemotherapy, leukocytic response to GMCSF or other cytokines should be taken into consideration.

ACKNOWLEDGMENTS

The authors thank Dr. Gayle Baldwin for critical advice, Jim Sayre for statistical assistance and Christine Wu for excellent technical assistance. This work was supported in part by grant NO1-CM-87289 from the National Cancer Institute and by the U.S. Department of Energy under contract DE-FC03-87ER60615.

REFERENCES

1. Gasson JC. Molecular physiology of granulocyte-macrophage colony stimulating factor. *Blood* 1991;7:1131–1145.
2. Begley CG, Nicola NA, Metcalf D. Proliferation of normal human promyelocytes and myelocytes after a single pulse stimulation by purified GM-CSF or G-CSF. *Blood* 1988;71:640–645.
3. Tomonaga M, Golde DW, Gasson JC. Biosynthetic (recombinant) human granulocyte-macrophage colony-stimulating factor: effect on normal bone marrow and leukemia cell lines. *Blood* 1986;67:31–36.
4. Demetri GD, Antman KH. Granulocyte-macrophage colony-stimulating factor (GM-CSF): preclinical and clinical investigations. *Semin Oncol* 1992; 19:362–385.
5. Kushner BH, Cheung NK. GM-CSF enhances 3F8 monoclonal antibody-dependent cellular cytotoxicity against human melanoma and neuroblastoma. *Blood* 1989;73:1936–1941.
6. Hamilton JA, Vairo G, Lingelbach SR. Activation and proliferation signals in murine macrophages: stimulation of glucose uptake by hemopoietic growth factors and other agents. *J Cell Physiol* 1988;134:405–412.
7. Hamilton JA, Vairo G, Lingelbach SR. CSF-1 stimulates glucose uptake in murine bone marrow-derived macrophages. *Biochem Biophys Res Commun* 1986;138:445–454.
8. Phelps ME, Huang SC, Hoffman EJ, Selin C, Sokoloff L, Kuhl DE. Tomographic measurement of local cerebral glucose metabolic rate in humans with (F-18)2-fluoro-2-deoxy-D-glucose: validation of method. *Ann Neurol* 1979;6:371–388.
9. Huang SC, Phelps ME, Hoffman EJ, Sideris K, Selin CJ, Kuhl DE. Noninvasive determination of local cerebral metabolic rate of glucose in man. *Am J Physiol* 1980;238:E69–82.
10. Sokoloff L, Reivich M, Kennedy C, et al. The [^{14}C]deoxyglucose method for the measurement of local cerebral glucose utilization: theory, procedure, and normal values in the conscious and anesthetized albino rat. *J Neurochem* 1977;28:897–916.
11. Som P, Atkins HL, Bandoypadhyay D, et al. A fluorinated glucose analog, 2-fluoro-2-deoxy-D-glucose (F-18): nontoxic tracer for rapid tumor detection. *J Nucl Med* 1980;21:670–675.
12. Hawkins RA, Hoh C, Dahlbom M, et al. PET cancer evaluations with FDG. *J Nucl Med* 1991;32:1555–1558.
13. Gritters LS, Francis IR, Zasadny KR, Wahl RL. Initial assessment of

positron emission tomography using 2-fluorine-18-fluoro-2-deoxy-D-glucose in the imaging of malignant melanoma. *J Nucl Med* 1993;34:1420–1427.
14. Hoh CK, Hawkins RA, Glaspy JA, et al. Cancer detection with whole-body PET using 2-[^{18}F]fluoro-2-deoxy-D-glucose. *J Comput Assist Tomogr* 1993; 17:582–589.
15. Kubota K, Matsuzawa T, Fujiwara T, et al. Differential diagnosis of lung tumor with positron emission tomography: a prospective study. *J Nucl Med* 1990;31:1927–1932.
16. Wahl RL, Kaminski MS, Ethier SP, Hutchins GD. The potential of 2-deoxy-2[^{18}F]fluoro-D-glucose (FDG) for the detection of tumor involvement in lymph nodes. *J Nucl Med* 1990;31:1831–1835.
17. Newman JS, Francis IR, Kaminski MS, Wahl RL. Imaging of lymphoma with PET with 2-[F-18]-fluoro-2-deoxy-D-glucose: correlation with CT. *Radiology* 1994;190:111–116.
18. Tse NY, Hoh CK, Hawkins RA, et al. The application of positron emission tomographic imaging with fluorodeoxyglucose to the evaluation of breast disease. *Ann Surg* 1992;216:27–34.
19. Hawkins RA, Choi Y, Huang SC, Messa C, Hoh CK, Phelps ME. Quantitating tumor glucose metabolism with FDG and PET. *J Nucl Med* 1992; 33:339–344.
20. Ichiya Y, Kuwabara Y, Otsuka M, et al. Assessment of response to cancer therapy using fluorine-18-fluorodeoxyglucose and positron emission tomography. *J Nucl Med* 1991;32:1655–1660.
21. Wahl RL, Zasadny K, Helvie M, Hutchins GD, Weber B, Cody R. Metabolic monitoring of breast cancer chemohormonotherapy using positron emission tomography: initial evaluation. *J Clin Oncol* 1993;11:2101–2111.
22. Rege SD, Chaiken L, Hoh CK, et al. Change induced by radiation therapy in FDG uptake in normal and malignant structures of the head and neck: quantitation with PET. *Radiology* 1993;189:807–812.
23. Patlak CS, Blasberg RG, Fenstenmacher JD. Graphical evaluation of blood-to-brain transfer constants from multiple-time uptake data. *J Cereb Blood Flow Metab* 1983;3:1–7.
24. Messa C, Choi Y, Hoh CK, et al. Quantification of glucose utilization in liver metastases: parametric imaging of FDG uptake with PET. *J Comput Assist Tomogr* 1992;16:684–689.
25. Hoh CK, Dahlbom M, Harris G, et al. Automated iterative three-dimensional registration of positron emission tomography images. *J Nucl Med* 1993;34:2009–2018.
26. Naeim F, Champlin R, Nimer S. Bone marrow changes in patients with refractory aplastic anemia treated by recombinant GM-CSF. *Hematol Pathol* 1990;4:79–85.
27. Aglietta M, Piacibello W, Sanavio F, et al. Kinetics of human hemopoietic cells after in vivo administration of granulocyte-macrophage colony stimulating factor. *J Clin Invest* 1989;83:551–557.
28. Groopman JE, Mitsuyasu RT, DeLeo MJ, Oette DH, Golde DW. Effect of recombinant human granulocyte-macrophage colony-stimulating factor on myelopoiesis in the acquired immunodeficiency syndrome. *N Engl J Med* 1987;317:593–598.
29. Abdel-Dayem HM, Sanchez J, al-Mohannadi S, Kempf J. Diffuse thallium-201-chloride uptake in hypermetabolic bone marrow following treatment with granulocyte stimulating factor. *J Nucl Med* 1992;33:2014–2016.
30. Stokkel MP, Valdes Olmos RA, Hoefnagel CA, Richel DJ. Tumor and therapy associated abnormal changes on bone scintigraphy. Old and new phenomena. *Clin Nucl Med* 1993;18:821–828.
31. Berlangieri SU, Peters WP, Coleman RE. Distribution of ^{99m}Tc-sulphur colloid during granulocyte colony-stimulating factor administration in autologous bone marrow transplantation. *Nucl Med Commun* 1993;14:896–901.
32. Fletcher BD, Wall JE, Hanna SL. Effect of hematopoietic growth factors on MR images of bone marrow in children undergoing chemotherapy. *Radiology* 1993;189:745–751.